Supplemental material

Table S1. Primers used in this study

Fig S1. Schematic of the generation of DNA-construct used to generate the transgenic line *OVA::Hep17$_{hep17}$*

Schematic representation of the *hep17* gene locus and the generation of the DNA construct used to generate *OVA::Hep17$_{hep17}$*. OVA (blue) is fused to *hep17* coding sequence (bright yellow box; signal peptide, yellow hatched box) under the control of the *hep17* 5'-UTR promoter and 3' terminus (light yellow boxes). The two *230p* targeting sequences (hatched boxes) flank the OVA expression cassette (see also Material and Methods). The position of *hep17* gene relative to start codon ($^{+}$/- bp), primers (**Table S1**) and restriction sites used are shown. SacII sites (red) were introduced to linearize the vector pL1884 prior to transfection.

Fig S2. Characterisation of OVA expression in different transgenic *P. berghei* NK65 and ANKA lines.

(A) Schematic representation of the *230p* locus in the reference *P. berghei* NK65 (GIMO$_{PbNK65}$) mother line and the two OVA-expressing transgenic lines. The GIMO$_{PbNK65}$ has the positive and negative selectable marker cassette (h*dhfr*::y*fcu*, black box) inserted into *P. berghei* NK65 *230p* locus. The OVA-expression cassettes were introduced into *230p* by double cross-over homologous recombination using the gene

targeting regions (hatched boxes) using GIMO transfection method. The *OVA$_{hsp70}$* line (2169cl1) encodes unconjugated full-length ovalbumin (ova; blue box) under the control of 5'-(promoter) and 3'-(terminator) UTRs of the *P. berghei hsp70* gene (grey boxes); The *OVA::mCherry$_{hsp70}$* line (2170cl1;) encodes OVA which is C-terminally fused to mCherry (red box) under the control of 5'-UTR of *hsp70* and the 3'-UTR of *dhfr/ts* (white box). The direction of transcription is indicated by the arrows.

(B) Southern analyses of PFG-separated chromosomes confirm the integration of the constructs into the *230p* locus on chromosome 3 of the two transgenic NK65 lines, resulting in the removal of the h*dhfr*::y*fcu* selection cassette. Hybridization was performed with a mixture of two probes, a control probe recognizing *p25* on chromosome (Chr.) 5 and a h*dhfr* probe recognizing h*dhfr*::y*fcu* on chromosome 3.

(C) Northern blot analysis of OVA-transgene transcription in purified schizonts of the two transgenic NK65 lines. Blots were hybridized using a PCR probe recognizing *ova* (primers 6466/6467, **Table S1**). As a loading control an oligonucleotide probe L644R was used that recognizes the large subunit (*lsu*) rRNA. wt, wild-type *P. berghei* NK65 parasites.

(D) Western analysis of OVA-expression in purified schizonts in the two transgenic NK65 lines. Blots were stained with anti-OVA antibodies. Anti-HSP70 antibody staining was used as a loading control. wt, wild-type *P. berghei* NK65 parasites.

(E) Western analysis (long exposure) confirming OVA-expression in purified schizonts of 2 different clones (cl.1 and cl.2) of transgenic *P. berghei* ANKA *OVA$_{hsp70}$* parasites (OVA).

Blots were stained with anti-OVA antibodies and anti-HSP70 antibody as a loading control.

(F) Western analysis indicates that a fraction of fusion protein OVA::mCherry expressed in PbANKA *OVA::mCherry*$_{hsp70}$ line (OVA::mC) is truncated because of a specific cleavage within mCherry. Western blots were prepared from proteins extracted from RBC infected with schizonts of OVA::mC or OVA::Hep17 (*OVA::Hep17*$_{hep17}$) lines, and stained with anti-OVA (left) and anti-mCherry (right) antibodies. Black arrows indicate full-length OVA::mCherry (~75KDa) recognised by both anti-OVA and anti-mCherry antibodies. Anti-OVA antibody also recognised a truncated version of OVA::mC protein (~55KDa, white arrow). A ~20kDa band (red arrow) showing the remainder of the OVA::mC protein was recognised by anti-mCherry antibody indicating that in a fraction of the fusion protein a specific cleavage had occurred within mCherry. OVA::Hep17 line is included as a control and single full length band (~62kDa) is visible only when the blot was probed with anti-OVA antibodies.

(G) The level of OVA-expression in synchronized blood stages of *OVA::Hep17*$_{hep17}$ and *OVA::mCherry*$_{hsp70}$ parasites. Trophozoites (Troph; 12-16 hours post invasion) and immature schizonts (Imm. Schiz; 18-22 hours post invasion) were obtained from synchronised infections. Western blots were stained with anti-OVA antibodies and anti-HSP70 antibodies as a loading control. Relative OVA expression level was calculated as the ratio between Western staining intensities of OVA and HSP70, which were quantified using Image J.

Fig S3. The course of blood stage infection (parasitemia and ECM) in mice infected with the different *P. berghei* ANKA lines.

(A) Parasitemia (% of infected erythrocytes) in tail blood of mice infected with 10^4 parasitised RBC (pRBC) of different *P. berghei* ANKA lines, $GIMO_{ANKA}$ (wild-type control), OVA_{hsp70} (OVA), $OVA::mCherry_{hsp70}$ (OVA::mC), $OVA::Hep17_{hep17}$ (OVA::Hep17). The results are the mean +/- SEM of a minimum of 2 separate experiments with a minimum total of 8 mice per group. **(B)** Kinetics of development of experimental cerebral malaria (ECM) shown as percentage of survival of mice infected with 10^4 pRBC of different PbANKA lines. ECM was defined as stage 4 or 5 of the clinical scale of ECM symptoms (see Materials and Method section) and the animals were euthanized when observed at stage 4 or 5. The results are from 2 separate experiments with a minimum total of 8 mice per group.

Fig S4. The location of OVA expression in blood stage parasites influences the activation of OVA-specific T cells during early stage of infection.

10,000 naïve $CD45.1^+$OT-I and 250,000 naïve $CD45.1^+$OT-II cells were adoptively transferred into $CD45.2^+$C57BL/6 mice one day prior to infection (10^4 pRBC i.v.) with different *P. berghei* ANKA lines, $GIMO_{ANKA}$ (control), OVA_{hsp70} (OVA), $OVA::mCherry_{hsp70}$ (OVA::mC), $OVA::Hep17_{hep17}$ (OVA::Hep17).

(A) Representative flow cytometric plots of total and donor $CD4^+$ and $CD8^+$ T cells in spleens of mice infected with different *P. berghei* ANKA lines at day 4 after infection. Hierarchal gating of total splenic $CD4^+$ and $CD8^+$ T cells (top row); host $CD45.1^-CD4^+$ T

cells and donor OVA-specific CD45.1$^+$CD4$^+$ OT-II cells (middle row); host CD45.1$^-$CD8$^+$ T cells and donor OVA-specific CD45.1$^+$CD8$^+$ OT-I cells (bottom row). **(B)** Percentages and absolute numbers (mean +/- SEM) of total and donor (OT-I/O-TII) T cells in spleens of mice (n=4) infected with different *P. berghei* ANKA lines at day 4 after infection. There was no significant expansion of total splenic T cells (left 4 graphs) nor OVA-specific OT-I or OT-II cells during infection with any of the *P. berghei* ANKA lines (right 4 graphs). The results are representative of 2 separate experiments. **(C)** Percentages and absolute numbers (mean +/- SEM) of donor (OT-II) T cells in spleens of mice (n=4) infected with different *P. berghei* ANKA lines at day 4 after infection. The activation of CD4$^+$CD45.1$^+$ OT-II cells was determined by examining the expression of CD69, CD25, Ki67, CD44 and CD62L. The results are representative of 2 separate experiments. *= $p<0.05$; **= $p<0.01$; ***= $p<0.001$.

Fig S5. Comparison of the endogenous splenic T cell responses in mice infected with the different *P. berghei* ANKA lines.

10,000 naïve CD45.1$^+$OT-I and 250,000 naïve CD45.1$^+$OT-II cells were adoptively transferred into CD45.2$^+$C57BL/6 mice one day prior to infection with the different *P. berghei* ANKA lines (10^4 pRBC i.v.), $GIMO_{ANKA}$ (control), OVA_{hsp70} (OVA), $OVA::mCherry_{hsp70}$ (OVA::mC), $OVA::Hep17_{hep17}$ (OVA::Hep17). The mean percentages of activated endogenous (recipient CD45.1$^-$) T cells was calculated in the spleens of mice (n=4) infected with different *P. berghei* ANKA lines on Day 4 and Day 6 of infection. T cell activation was assessed by examining the expression of CD69, CD25, CD44 and CD62L

and proliferation was assessed through expression of Ki67. The results are the mean +/- SEM of the group with 4 mice per group and are representative of 2 separate experiments. *= p<0.05; **= p<0.01; ***= p<0.001.

Fig S6. Comparison of the endogenous intracerebral T cell responses in mice infected with the different *P. berghei* ANKA lines.

10,000 naïve CD45.1^{+}OT-I and 250,000 naïve CD45.1^{+}OT-II cells were adoptively transferred into CD45.2^{+}C57BL/6 mice one day prior to infection with the different *P. berghei* ANKA lines (10^{4} pRBC i.v.), $GIMO_{ANKA}$ (control), OVA_{hsp70} (OVA), $OVA::mCherry_{hsp70}$ (OVA::mC), $OVA::Hep17_{hep17}$ (OVA::Hep17). The mean percentages of activated endogenous (recipient CD45.1^{-}) T cells was calculated in the brains of mice (n=4) infected with different *P. berghei* ANKA lines on Day 6 of infection, when infected mice developed ECM. T cell activation was assessed by examining the expression of CD69, CD25, CD44 and CD62L and proliferation was assessed through expression of Ki67. The results are the mean +/- SEM of the group with 4 mice per group and are representative of 2 separate experiments. *= p<0.05; **= p<0.01; ***= p<0.001.

Table S1. Primers used in this study

No.	Primer sequences	Restriction sites	Description
Primers for construct generation			
6464	CCGCGGATCCATGGGCTCCATCGGTGCAG	*Bam*HI	OVA, F
6465	GCGCCACCGGCGACTCAAGGGGAAACACATCTG	*Sgr*AI	OVA, R
6466	CCCGCTCGAGATGGGCTCCATCGGTGCAG	*Xho*I	OVA, F
6467	CCGCGGATCCAGGGGAAACACATCTGCC	*Bam*HI	OVA, R
6920	GCGCAATTCCATATGATGGGCTCCATCGGTGCAG	*Nde*I	OVA, F
6659	ATAAGAATGCGGCCGCTGTCAATAATATTTATTTTGGTACAC	*Not*I	5'*hep17*, F
6660	GCGAATTCCATATGTTTATTTTTTCCATAAGCATTG	*Nde*I	*hep17*, R
6661	GCGGGATCCGGGATCGATGGTAAAACTGGCTCCAAAAATG	*Bam*HI, *Cla*I	*hep17*, F
6662	CGGGGTACCATTGTTTGTGGTCATAACATAG	*Kpn*I	3'*hep17*, R
6838	CCCGCTCGAGCCGCGGTATATGGTAAAGAACCTACTAACAC	*Xho*I, *Sac*II	5'*230p*, F
6839	CCCGGAATTCAGGATGTGTTTTATTTGGATGTG	*Eco*RI	5'*230p*, R
5587	CCGGGGTACCAATTCTCTTGAGCCCGTTAATG	*Kpn*I	3'*230p*, F
6840	CGGGGTACCGCGGCTATATTTTTGGTTTTATAATCTTCAC	*Kpn*I, *Sac*II	3'*230p*, R
Primers for probe generation			
886	GGAAGATCTATGGTTGGTTCGCTAAACTGCATCG		h*dhfr*, F
887	GGAAGATCTTTAATCATTCTTCTCATATACTTC		h*dhfr*, R
1462	CATGCCATGGATGAATACTTATTACAGTG		*p25*, F
1463	CCGGAATTCTTAAATGATATTTGAAAATATTAG GGAAACAGTCCATCTATAATTG		*p25*, R

F = forward primer, R= reverse primer
Red, restriction sites

Figure S1

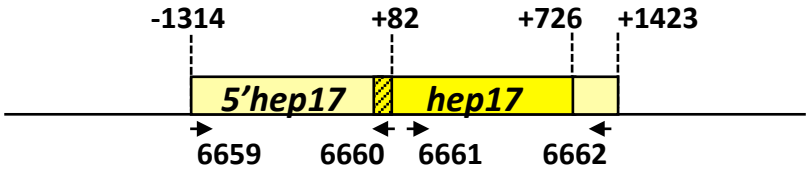

hep17 genomic locus
PBANKA_092670

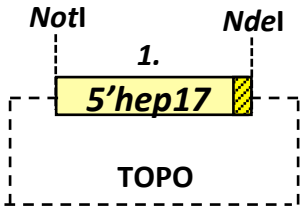

Intermediate vector constructed in pCR2.1-TOPO vector

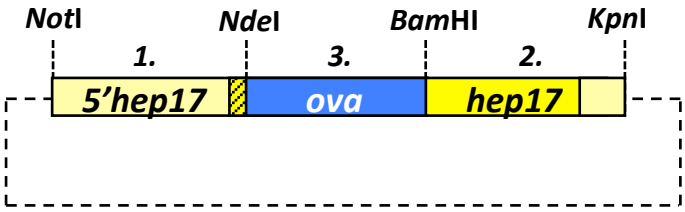

Intermediate vector constructed in pCR2.1-TOPO vector

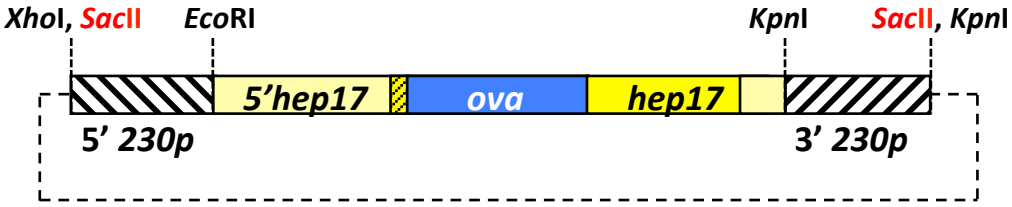

Final construct
pL1884

Figure S2

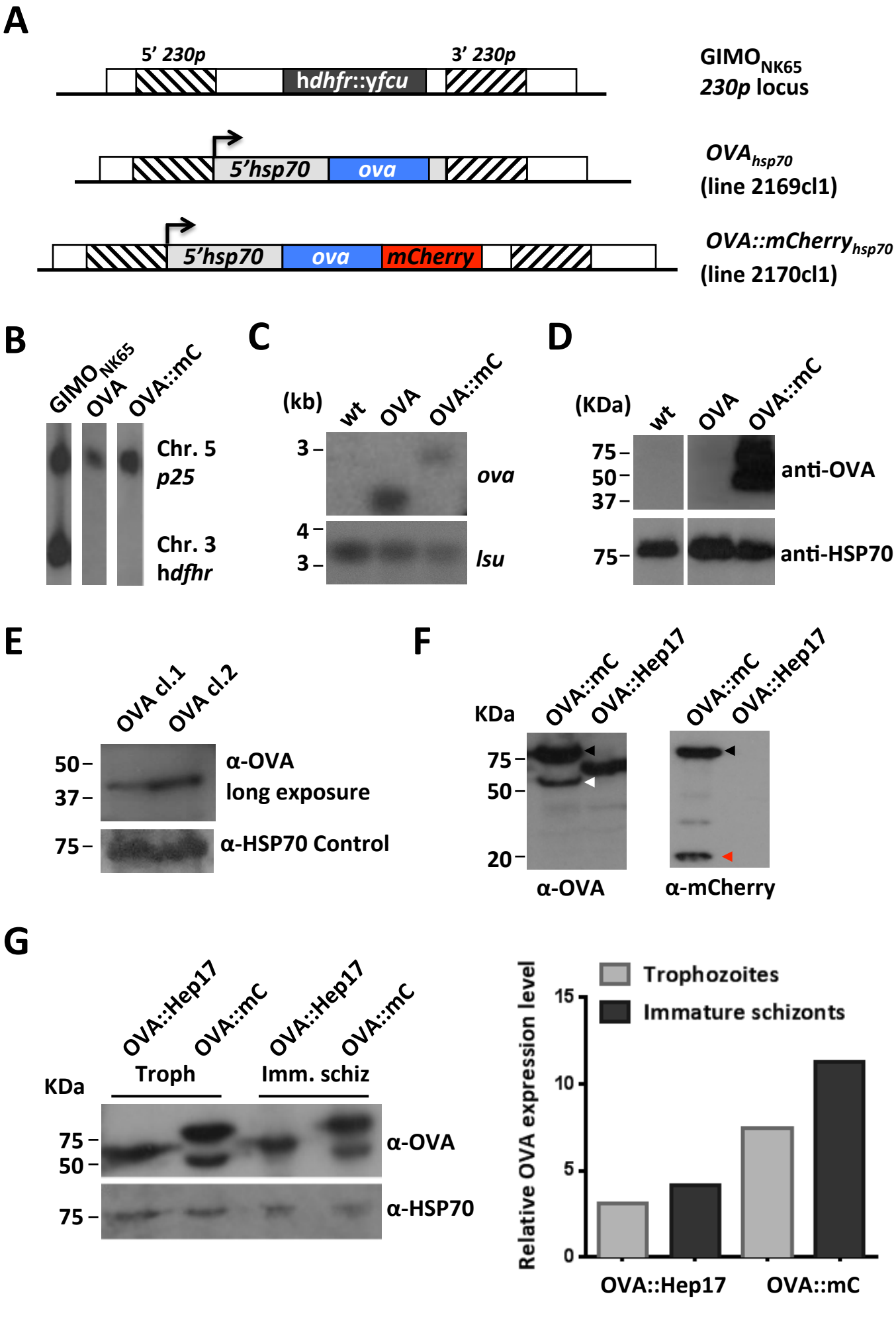
A
5' 230p
hdhfr::yfcu
3' 230p
GIMO NK65
230p locus
5'hsp70
ova
OVA hsp70
(line 2169cl1)
5'hsp70
ova
mCherry
OVA::mCherry hsp70
(line 2170cl1)
B
GIMO NK65
OVA
OVA::mC
Chr. 5
p25
Chr. 3
hdfhr
C
(kb)
wt
OVA
OVA::mC
3
ova
4
3
lsu
D
(KDa)
wt
OVA
OVA::mC
75
50
37
anti-OVA
75
anti-HSP70
E
OVA cl.1
OVA cl.2
50
37
α-OVA
long exposure
75
α-HSP70 Control
F
KDa
OVA::mC
OVA::Hep17
OVA::mC
OVA::Hep17
75
50
20
α-OVA
α-mCherry
G
OVA::Hep17
OVA::mC
OVA::Hep17
OVA::mC
KDa
Troph
Imm. schiz
75
50
α-OVA
75
α-HSP70
Trophozoites
Immature schizonts
Relative OVA expression level
15
10
5
0
OVA::Hep17
OVA::mC

Figure S3

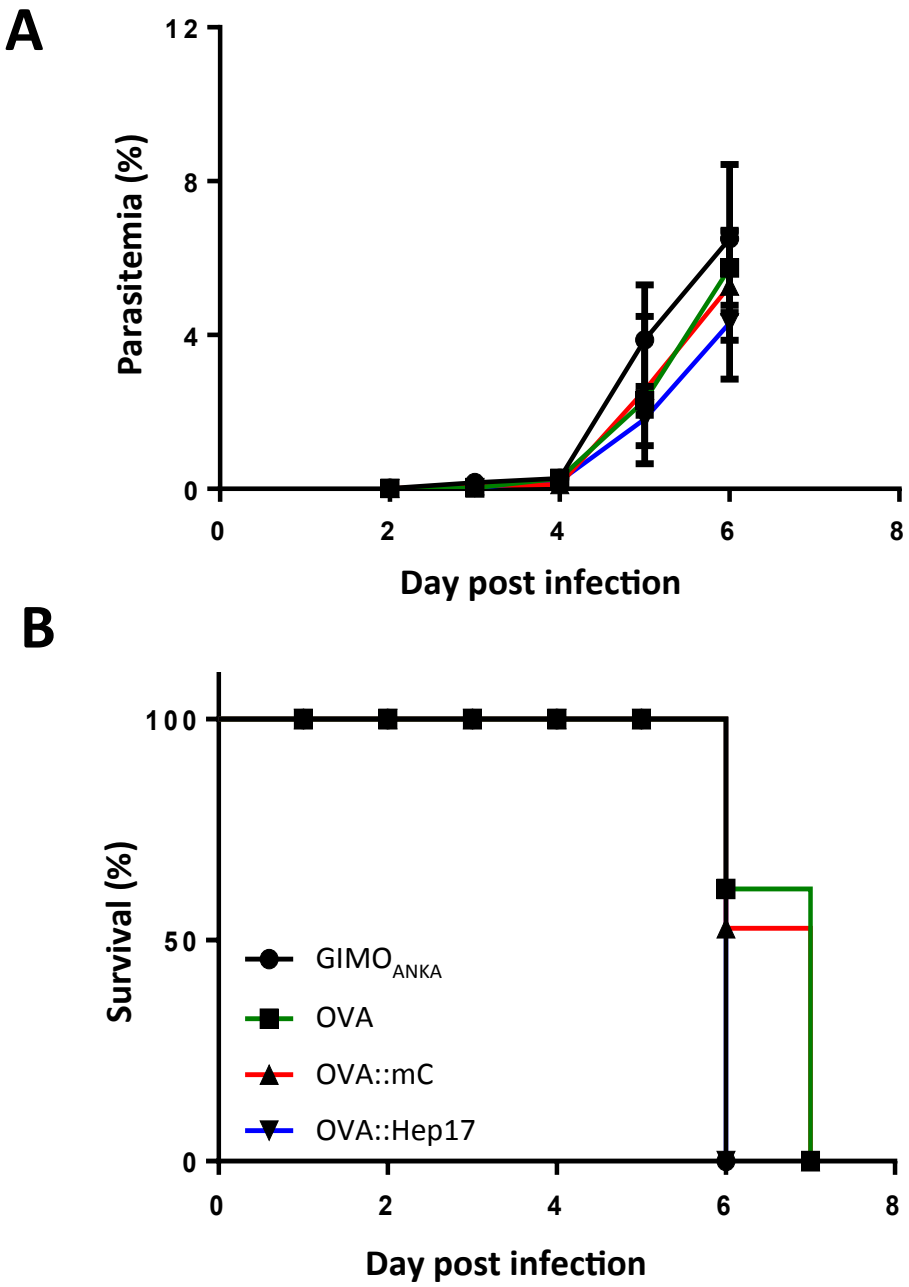
A
12
8
4
0
Parasitemia (%)
0
2
4
6
8
Day post infection
B
100
50
0
Survival (%)
GIMO$_{ANKA}$
OVA
OVA::mC
OVA::Hep17
0
2
4
6
8
Day post infection

Figure S4

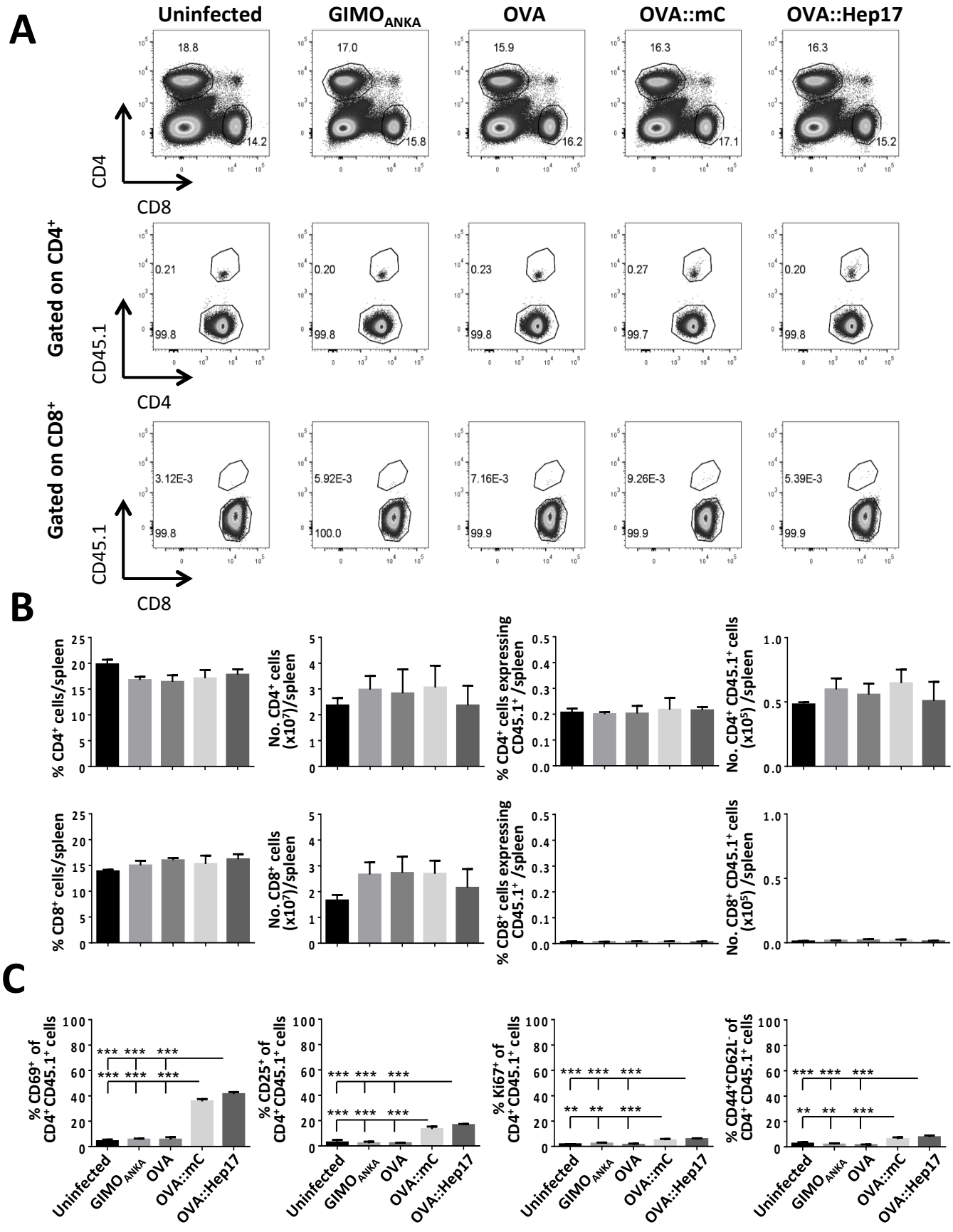
A
Uninfected
GIMO$_{ANKA}$
OVA
OVA::mC
OVA::Hep17
CD4
CD8
CD45.1
Gated on CD4$^+$
Gated on CD8$^+$
B
% CD4$^+$ cells/spleen
No. CD4$^+$ cells (x10^7)/spleen
% CD4$^+$ cells expressing CD45.1$^+$ /spleen
No. CD4$^+$ CD45.1$^+$ cells (x10^5) /spleen
% CD8$^+$ cells/spleen
No. CD8$^+$ cells (x10^7)/spleen
% CD8$^+$ cells expressing CD45.1$^+$ /spleen
No. CD8$^+$ CD45.1$^+$ cells (x10^5) /spleen
C
% CD69$^+$ of CD4$^+$CD45.1$^+$ cells
% CD25$^+$ of CD4$^+$CD45.1$^+$ cells
% Ki67$^+$ of CD4$^+$CD45.1$^+$ cells
% CD44$^+$CD62L$^-$ of CD4$^+$CD45.1$^+$ cells

Figure S5

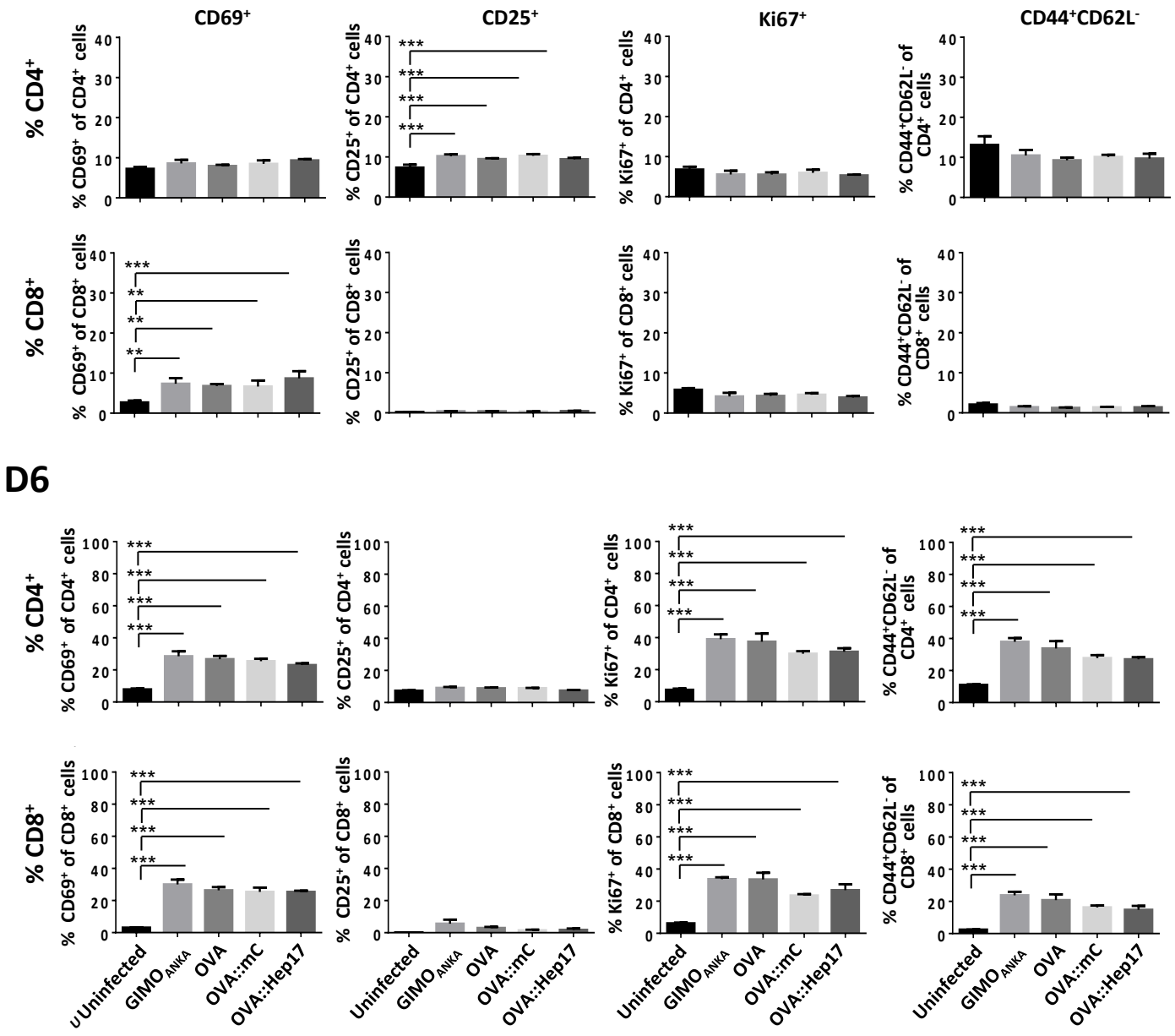
D4
CD69+
CD25+
Ki67+
CD44+CD62L-
% CD4+
% CD8+
% CD69+ of CD4+ cells
% CD25+ of CD4+ cells
% Ki67+ of CD4+ cells
% CD44+CD62L- of CD4+ cells
% CD69+ of CD8+ cells
% CD25+ of CD8+ cells
% Ki67+ of CD8+ cells
% CD44+CD62L- of CD8+ cells
D6
Uninfected
GIMOANKA
OVA
OVA::mC
OVA::Hep17

Figure S6

D6

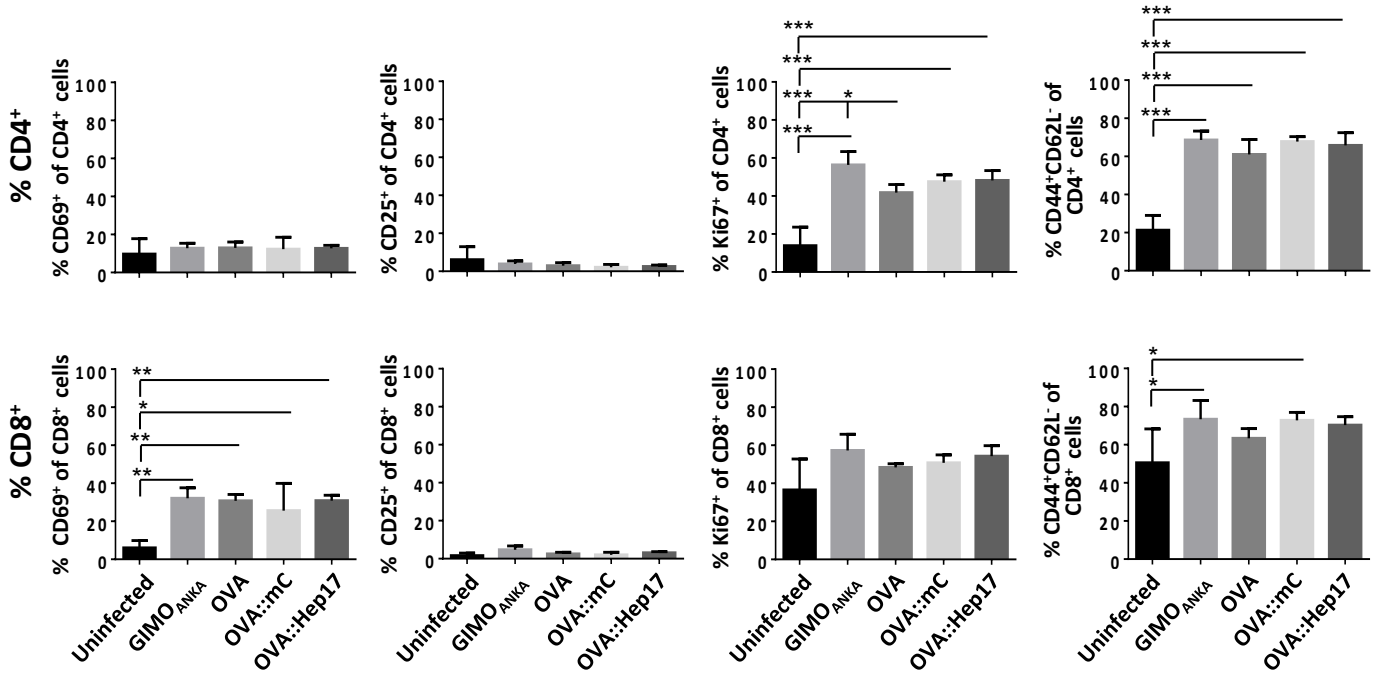
% CD4+
% CD69+ of CD4+ cells
% CD25+ of CD4+ cells
% Ki67+ of CD4+ cells
% CD44+CD62L- of CD4+ cells
% CD8+
% CD69+ of CD8+ cells
% CD25+ of CD8+ cells
% Ki67+ of CD8+ cells
% CD44+CD62L- of CD8+ cells
Uninfected
GIMOANKA
OVA
OVA::mC
OVA::Hep17